

PII: S0038–1098(96)00681-3

## OBSERVATION OF JOSEPHSON VORTEX LATTICE MELTING IN A HIGHLY ANISOTROPIC SUPERCONDUCTOR

M.S. Fuhrer,<sup>a</sup> K. Ino,<sup>b</sup> K. Oka,<sup>b</sup> Y. Nishihara<sup>b</sup> and A. Zettl<sup>a</sup><sup>a</sup>Department of Physics, University of California at Berkeley and Materials Sciences Division, Lawrence Berkeley Laboratory, Berkeley, CA 94720, U.S.A.<sup>b</sup>Electrotechnical Laboratory, Tsukuba, Ibaraki 305, Japan

(Received 28 October 1996 by S.G. Louie)

The Josephson vortex lattice state of the highly anisotropic high- $T_c$  superconductor  $\text{Bi}_2\text{Sr}_2\text{CaCu}_2\text{O}_8$  has been probed by measurements of the out-of-plane ( $c$ -axis) resistivity as a function of temperature, current density, magnetic field strength  $H$  and magnetic field orientation angle  $\theta$ . Anomalous dissipation is observed below a critical temperature identified as the melting transition of the Josephson vortex lattice. The critical  $T$ - $H$  and  $T$ - $\theta$  phase boundaries are determined. The melting transition is interpreted as a Kosterlitz–Thouless depairing of interlayer vortex/anti-vortex pairs. The same model accounts well for unusual in-plane dissipation observed previously in  $\text{Bi}_2\text{Sr}_2\text{CaCu}_2\text{O}_8$ . © 1997 Elsevier Science Ltd. All rights reserved

It has been proposed [1] that a sufficiently strong magnetic field applied parallel to the layers of a Josephson-coupled superconductor could destroy the phase coherence between layers but leave the individual layers superconducting, corresponding to melting of the Josephson vortex lattice. A more recent study [2] has found that, at least in the case of complete confinement of the field between the layers, Josephson vortex lattice melting would correspond to the full destruction of superconductivity, i.e.  $T_{\text{melt}} = T_c$ , with  $T_c$  the superconducting phase transition temperature. An intriguing possibility is thus the observable melting of a Josephson vortex lattice in a system where the vortices are not strictly confined between the layers.

We have explored the possibility of Josephson vortex lattice melting in a coupled layered superconductor by performing detailed out-of-plane ( $c$ -axis) d.c. transport measurements on the highly anisotropic superconductor  $\text{Bi}_2\text{Sr}_2\text{CaCu}_2\text{O}_8$  (BSCCO) in the Josephson vortex state with the magnetic field  $H$  oriented parallel to the superconducting layers ( $H \parallel ab$ -plane). In this state the flux vortices reside primarily but not exclusively in the regions between the superconducting layers. We find that the electric field-current density  $E(J)$  characteristics of the  $c$ -axis resistivity  $\rho_c$  change from ohmic to non-ohmic at a well-defined critical temperature somewhat below  $T_c$ . We associate this critical temperature with the

melting transition of the Josephson vortex lattice. The dependence of the melting transition on the magnitude and orientation of  $H$  allow the critical phase boundaries to be mapped out. These boundaries are inconsistent with conventional vortex lattice melting. Instead, we interpret the melting of the Josephson vortex lattice as a Kosterlitz–Thouless (KT) depairing of interlayer vortex/anti-vortex pairs. The same KT vortex-melting model accounts in a consistent way for unusual in-plane dissipation observed previously in BSCCO for  $H$ -fields oriented parallel to the  $ab$ -plane.

The single crystals of BSCCO used for this study were grown by a traveling-solvent floating-zone technique described elsewhere [3]. Several samples were measured with similar results. Data presented here are all for the same crystal with dimensions  $0.70 \text{ mm} \times 1.80 \text{ mm} \times 20 \mu\text{m}$ ; the smallest dimension represents the  $c$ -axis. Silver paint pads were applied to the top and bottom  $ab$ -plane facets of the sample. The sample was then annealed in air at  $700^\circ\text{C}$  for 30 min, after which gold wires were affixed to the silver pads with silver paint. Contact resistances were  $< 1 \Omega$ . The resistivity of the sample was measured using a standard four-probe technique. A variable d.c. current was applied to the sample and the voltage measured using a d.c. nanovoltmeter (Keithley 182). The resistivity

measurements were averaged over both current directions to eliminate thermal EMFs. The sample was mounted in a superconducting magnet cryostat with a rotating stage which allowed *in-situ* tilting and alignment of the sample with respect to the magnetic field with an angular resolution of  $0.013^\circ$ . Temperature accuracy was  $\pm 30$  mK. The  $H = 0T_c$  was 85.5 K, as determined by the onset of non-linearity in the *c*-axis resistivity.

Figure 1 shows  $\rho_c$  in BSCCO as a function of temperature for two different measuring current densities, in the presence of an in-plane ( $H \parallel ab$ ) field  $H = 7.5$  T. The general field-induced broadening of the resistive transition below  $T_c$  is consistent with previous studies [4]. However, Fig. 1 shows that the high and low current density data are identical only for temperatures  $T$  above a critical temperature  $T^*$ ; below  $T^*$  the data sets diverge. The high current density curve is smooth near  $T^*$ , while the low current density curve shows a kink at  $T^*$  below which the low current resistivity drops precipitously. Electric field as a function of current density [ $E(J)$ ] curves collected at temperatures above and below  $T^*$  show distinctly different behavior. For  $T > T^*$  the  $E(J)$  characteristics are ohmic (i.e. always linear), while for  $T < T^*$  the  $E(J)$  characteristics are non-ohmic, displaying a well-defined critical current for the onset of dissipation with  $E \propto (J - J_{\text{crit}})$  for  $J > J_{\text{crit}}$  where  $J_{\text{crit}}$  is the critical current. The upper inset in Fig. 1 shows examples of the  $E(J)$  characteristics for  $T$  above and below  $T^*$ .  $J_{\text{crit}}$  is temperature-dependent in the state  $T < T^*$  and increases roughly linearly with decreasing temperature, as shown in the lower inset to

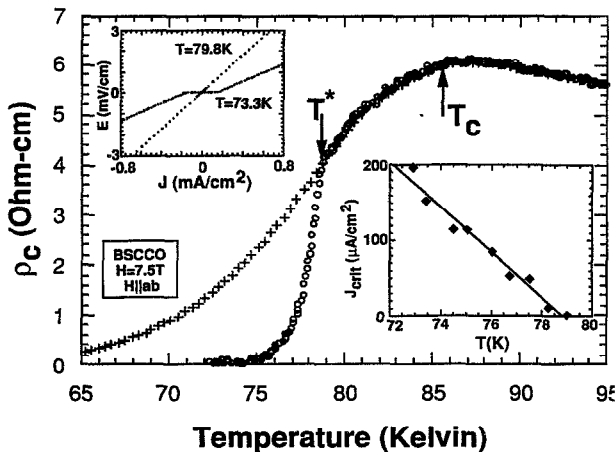


Fig. 1.  $\rho_c$  vs  $T$  for BSCCO with  $H = 7.5$  Tesla  $\parallel ab$ . Crosses and circles represent measuring current densities of  $8 \times 10^{-2}$  and  $4 \times 10^{-5}$  A  $\text{cm}^{-2}$ . The low current density resistivity falls sharply below a kink at  $T^* = 78.9$  K. The upper inset shows the electric field-current density relationship  $E(J)$  at  $T = 79.8$  K and 73.3 K, above and below  $T^*$ , respectively. The lower inset shows  $J_{\text{crit}}$  vs  $T$ .

Fig. 1.  $T^*$  is equivalently defined by the kink in the low current resistance or the appearance of a finite critical current in the  $E(J)$  characteristics. For the  $H = 7.5$  T data in Fig. 1,  $T^* = 78.9$  K, significantly below  $T_c = 85.5$  K.

The kink in the low current resistivity seen in Fig. 1 is reminiscent of the kink in both the in-plane and *c*-axis resistivities vs temperature observed in  $\text{YBa}_2\text{Cu}_3\text{O}_7$  (YBCO) crystals, with the magnetic field parallel or perpendicular to the *ab*-plane [5, 6]. It is noteworthy that in YBCO the dissipation kink is clearly observable at a current density of 4 A  $\text{cm}^{-2}$ , while in the configuration described here for BSCCO the kink is only apparent at much lower current densities, on the order of  $10^{-4}$  A  $\text{cm}^{-2}$ . In the case of YBCO, the kink corresponds to melting of the Abrikosov vortex lattice or glass, with  $E(J)$  characteristics ohmic above and non-ohmic below the melting temperature. Below the kink in YBCO  $\rho_c$  in YBCO is observed to follow a scaling law with the melting temperature as the relevant temperature scale. In BSCCO, for temperatures  $T < T^*$ , our  $\rho_c$  data in the high current density limit obey well a scaling functional form [7]  $\rho(T) = \rho_0 \exp [(1 - T/T^*)^\alpha / TH^\beta]$  with fixed  $\alpha$ ,  $\beta$  and  $\rho_0$ , over the entire range of applied magnetic fields [8]. Such a scaling is suggestive of dissipation due to flux creep of a frozen vortex lattice [9] and the success of the parameter  $T^*$  as opposed to  $T_c$  in scaling the resistivity supports the identification of  $T^*$  as a phase transition within the vortex state, similar to the case of YBCO.

We suggest that  $T^*$  is the Josephson vortex lattice melting temperature in BSCCO. As such,  $T^*$  is expected to have sensitive and unique functional dependences on the magnetic field magnitude and orientation which distinguish it from the melting transition [10] of more conventional (Abrikosov or pancake) flux lattices in BSCCO. We have repeated the resistivity measurements described in Fig. 1 for different  $H$  and for finite misalignment angle  $\theta$ , thus identifying the critical  $T$ - $H$  and  $T$ - $\theta$  phase boundaries.

Figure 2 shows the critical field  $H^*$  necessary to induce melting as a function of temperature in BSCCO, again with  $H$  aligned with the *ab*-plane (i.e.  $\theta = 0$ ).  $H^*(T)$  divides the phase diagram into Josephson vortex solid and liquid. The upper critical field  $H_{c2}(T)$  is also shown (for a conservative estimate of 45 Tesla  $\text{K}^{-1}$  [11]) and is nearly vertical on this scale. As expected,  $H^*$  decreases smoothly with increasing  $T$ . For fields  $H < 2$  T we were not able to clearly resolve  $T^*$ ; however, the data strongly suggest  $T^*(H = 0) \cong 83.1$  K, roughly 2 K below  $T_c$ .

Figure 3 shows  $\rho_c$  in BSCCO for two different measuring current densities, as a function of  $\theta$ , the angle between the applied  $H$  field and the *ab*-plane of

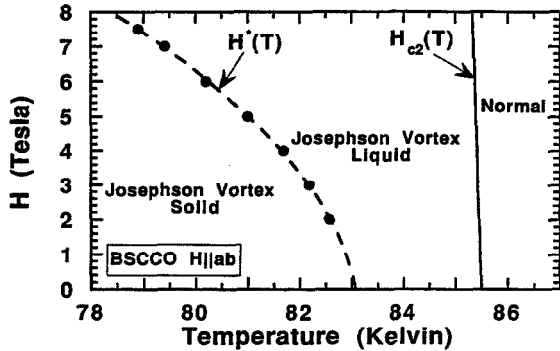


Fig. 2.  $H$ - $T$  phase diagram for BSCCO with  $H\parallel ab$ . Filled circles represent the experimentally measured points  $T^*(H)$ . The dashed line  $H^*(T)$  is a guide to the eye for the Josephson vortex melting line. The data extrapolate to  $T^*(H=0)$  @ 83.0 K. The upper critical field  $H_{c2}(T)$  is also shown.

the crystal. For all data shown in the figure  $T = 73.3$  K and  $H = 7.5$  T. Non-ohmic dissipation is observed only within a very small angular window of order  $1^\circ$  centered on  $\theta = 0$ . Within this window there is an extreme sensitivity of  $\rho_c$  on  $\theta$  for low current densities. This sensitivity may be used to set an upper bound on any possible  $c$ -axis mosaic spread in this crystal of  $< 0.2$  degrees. For high current densities a novel “bump” feature is observed [12] and the dissipation is somewhat enhanced close to  $\theta = 0$ . The “splitting” of the high and low current density data in Fig. 3 at a well-defined angle identifies  $T^*$  at that critical angle: from Fig. 3,  $T^*(\theta = 0.80^\circ) = 73.3$  K. The general trough in the resistivity for  $|\theta| > 1^\circ$  may be explained by the disappearance of the perpendicular component of the magnetic field, which is the source of the much larger dissipation observed [13] for  $H\parallel c$ . This Lorentz force independent dissipation has been explained in terms of a reduction of the Josephson junction area [14] or weak

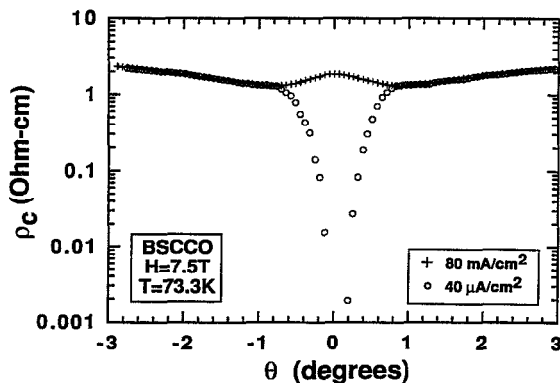


Fig. 3.  $\rho_c$  vs field misalignment angle  $\theta$  at  $T = 73.3$  K for two current densities.

link creation [4] by the component of  $H\parallel c$ . The high current density hump near  $|\theta| < 1^\circ$  must then correspond to Lorentz force dissipation, i.e. dissipation for Josephson vortices parallel to the  $ab$ -plane. The dominance of Lorentz force dissipation in the same angular range that contains  $T^*$  is evidence that  $T^*$  is a property of the Josephson vortices.

We have measured  $\rho_c(T)$  at different fixed angular orientations, allowing the determination of  $T^*(\theta, H = 7.5$  T). The resulting  $T$ - $\theta$  phase boundary is shown in Fig. 4. We find a reasonable fit to the experimental data by an empirical parabolic dependence on the field component perpendicular to the layers, i.e.  $T^*(\theta) = T^*(\theta = 0) + A[H \sin \theta]^2$  (solid curve in Fig. 4). This demonstrates a particularly strong suppression of the melting transition temperature by an out-of-plane component of the  $H$  field. We also note that  $T^*$  does not approach  $T_c$  as  $\theta \rightarrow 0$ . This again verifies that we are measuring a property of the Josephson vortex lattice and not an effect due to a misalignment of the field. Furthermore, the steep dependence of  $T^*$  on angle (the empirical  $\sin^2 \theta$  fit in Fig. 4 extrapolates to  $T^* = 0$  K at an angle of  $\sim 3.3^\circ$ ) is inconsistent with Abrikosov vortex melting, which is observed in BSCCO at  $\theta = 90^\circ$ , at low but finite temperatures [10].

In YBCO, conventional vortex lattice melting is well accounted for by the anisotropic effective-mass model which predicts [15, 16] for the flux melting temperature  $T_m$

$$[T_c - T_m] \propto H^{1/2} \epsilon^{1/4}(\theta), \quad (1)$$

where  $\epsilon = \cos^2(\theta) + \gamma^2 \sin^2(\theta)$  and  $\gamma$  is the mass anisotropy  $m_c/m_{ab}$ . The dashed curve in Fig. 4 shows equation (1) fit to the data for  $\gamma = 200$  and  $T_m(H = 0) = 79.5$  K. The fit is poor and cannot be improved by altering the value of  $\gamma$  or  $T_m(0)$ . The fact that the observed transition temperature  $T^*$  falls off more rapidly as a

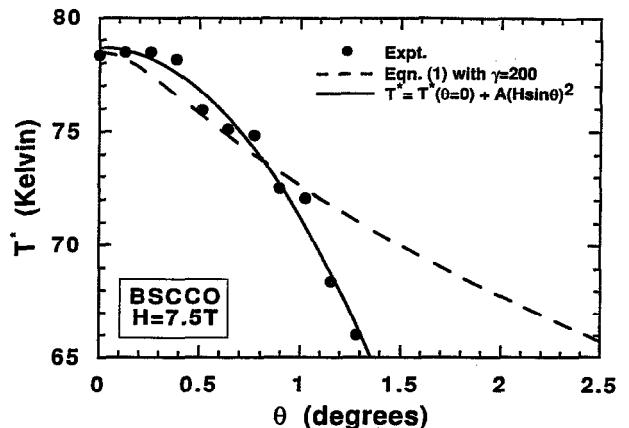


Fig. 4.  $T^*$  vs field misalignment angle  $\theta$  at  $H = 7.5$  Tesla. Fits to the data are described in the text.

function of angle than equation (1) predicts demonstrates the fundamental differences between Josephson vortex lattice melting and conventional vortex lattice melting. The presence of externally applied (finite angle) perpendicular fields are not the origin of  $T^*$  but serve only to sharply suppress the Josephson vortex melting transition.

As mentioned previously, a Josephson vortex lattice is not expected to melt in the limit of complete confinement to the space between the superconducting planes [2]. Complete confinement of the vortices within the planes also implies  $\rho_{ab} = 0$  for  $H \parallel ab$  and  $J \perp H$ , since in this configuration the Lorentz force is directed out of the plane. As this is contrary to experimental observations in BSCCO [17], the Josephson vortices here are not strictly confined. Josephson vortices parallel to the superconducting planes may cross the planes by the jog of a finite segment, which corresponds to the creation of a vortex/anti-vortex pair in the superconducting layer. Crossing by the entire flux line requires separation of the pair. This is reminiscent of Kosterlitz–Thouless [18] (KT) behavior: in thin superconductors there exists a temperature  $T_{KT}$  at which thermally excited vortex-antivortex pairs are dissociated [19, 20].

We propose that the KT transition and Josephson vortex lattice melting in BSCCO go hand-in-hand [21]. For  $H = 0$ , BSCCO undergoes a KT transition a few degrees below  $T_c$  [22], in agreement with  $T^*(H \rightarrow 0) \cong 83.1$  K observed in Fig. 2. For finite  $H \parallel ab$ , the presence of magnetic flux is predicted [23] to modify the interaction between vortex/anti-vortex pairs. In the case of a vortex solid the interface between pairs becomes linear in their separation, which effectively confines the pairs. In the case of a vortex liquid the interaction becomes logarithmic. The KT transition thus leads to a dissociation of the vortex/anti-vortex pairs, allowing for dislocations of the flux lattice across the superconducting planes and consequent melting of the Josephson vortex with the observed disappearance of the critical current. The phase boundary line of Fig. 2, then, defines not only  $T^*(H)$  but also  $T_{KT}(H)$  in BSCCO. The suppression of  $T^*(H)$  by the introduction of a perpendicular field component (Fig. 3) is consistent with the observation [24] of the suppression of  $T_{KT}$  in BSCCO by the application of  $H \parallel c$ .

The model of coupled Josephson vortex lattice melting and Kosterlitz–Thouless transition makes additional predictions for the in-plane dissipation ( $\rho_{ab}$ ) of BSCCO in the Josephson vortex state ( $H \parallel ab$ ), which we here compare to previous measurements.  $\rho_{ab}$  data should exhibit dissipation for  $H \parallel ab$  for current orientations parallel and perpendicular to  $H$ , since in both orientations there is a Lorentz force on the thermally excited pancake vortices. Below the melting temperature

vortex/anti-vortex pairs must be separated by the current, giving rise to the usual KT power-law  $E(J)$  relation. We thus expect a crossover from linear to power-law  $E(J)$   $\rho_{ab}$  characteristics in BSCCO as the temperature or field is reduced below the melting transition. Precisely this behavior has been observed experimentally [25], where the power law exponent  $a$  in the relation  $E \sim J^a$  is  $\approx 1$  at high applied  $H$  but begins to increase sharply at  $H = 2$  T for  $T = 80$  K. Although this crossover was originally attributed to a suppression of pair creation by the magnetic field, it appears to be instead related to a change in the pair interaction caused by melting of the flux lattice.

*Acknowledgements*—This work was supported in part by the Director, Office of Basic Energy Sciences, Materials Sciences Division of the U.S. Department of Energy under contract No. DE-AC03-76SF00098. AZ received support from the Miller Institute for Basic Research in Science.

## REFERENCES

1. Efetov, K.B., *Sov. Phys. JETP*, **49**, 1979, 905.
2. Korshunov, S.E. and Larkin, A.I., *Phys. Rev.*, **B46**, 1992, 6395.
3. Ha, D.H. *et al.*, *Bulletin of the Electrotechnical Laboratory*, **57**, 1993, 15.
4. Briceno, G., Crommie, M.F. and Zettl, A., *Physica*, **C204**, 1993, 389.
5. Charalambous, M., Chaussy, J. and Lejay, P., *Phys. Rev.*, **B45**, 1992, 5091.
6. Kwok, W.K. *et al.*, *Phys. Rev. Lett.*, **69**, 1992, 3370.
7. Kim, D.H. *et al.*, *Phys. Rev.*, **B42**, 1990, 6249.
8. Fuhrer, M.S. *et al.* To be published.
9. Tinkham, M., *Phys. Rev. Lett.*, **61**, 1988, 1658.
10. Schilling, A. *et al.*, *Phys. Rev. Lett.*, **71**, 1993; 1899, Zeldov, E. *et al.*, *Nature* **375**, 1995, 373; Cubitt, R. *et al.*, *Nature* **365**, 1993, 407.
11. Palstra, T.T.M. *et al.*, *Phys. Rev.*, **B38**, 1988, 5102.
12. A similar bump has been observed in the  $ab$ -plane resistivity. See Iye, Y. *et al.*, *Physica C174*, 1991, 227 and Chaparala, M. *et al.*, *Phys. Rev.* **B53**, 1996, 5818.
13. Briceno, G., Crommie, M.F. and Zettl, A., *Phys. Rev. Lett.*, **66**, 1991, 2164.
14. Gray, K.E. and Kim, D.H., *Phys. Rev. Lett.*, **70**, 1993, 1693.
15. Beck, R.G. *et al.*, *Phys. Rev. Lett.*, **68**, 1992, 1594.
16. Blatter, G., Geshkenbein, V.B. and Larkin, A.I., *Phys. Rev. Lett.*, **68**, 1992, 875.
17. Iye, Y., Nakamura, S. and Tamegai, T., *Physica*, **C159**, 1989, 433.
18. Kosterlitz, J.M. and Thouless, D.J., *J. Phys.*, **C6**, 1973, 1181.
19. Beasley, M.R., Mooij, J.E. and Orlando, T.P., *Phys. Rev. Lett.*, **42**, 1979, 1165.
20. Halperin, B.I. and Nelson, D.R., *J. Low. Temp. Phys.*, **36**, 1979, 599.

21. A connection between the  $T_{KT}$  and melting of the 2D Abrikosov lattice has been previously noted. See, for example, Fisher, D.S. *et al.*, *Phys. Rev.*, **B43**, 1991, 130.
22. Martin, S. *et al.*, *Phys. Rev. Lett.*, **62**, 1989, 677.
23. Blatter, G., Ivlev, B.I. and Rhyner, J., *Phys. Rev. Lett.*, **66**, 1991, 2392.
24. Artemenko, S.N., Gorlova, I.G. and Latyshev, Y.I., *Physica*, **193**, 1992, 47.
25. Ando, Y. *et al.*, *Phys. Rev. Lett.*, **67**, 1991, 2737.